

Position-Based Limited Feedback Scheme for Railway MU-MIMO Systems

Li Yan, *Student Member, IEEE*, Xuming Fang, *Member, IEEE*, and Cheng-Xiang Wang, *Senior Member, IEEE*

Abstract—In future railway communications, the system architecture is highly likely to be based on the mobile relay structure. However, during the transition period, onboard passenger equipment can only directly connect to wayside public mobile networks to get wireless services. As an efficient technology to increase the capacity widely used in Long-Term Evolution (LTE) public mobile networks, multiuser multiple input–multiple output (MU-MIMO) requires channel state information (CSI) of users at base stations to suppress interuser interference, which poses a bandwidth burden on feedback links. Thus, how to reduce the MU-MIMO feedback load becomes an urgent problem. In railway scenarios, onboard passenger equipment of a user set almost has the same signal-to-noise ratio (SNR), which provides a new way to reduce the MU-MIMO feedback overheads. Accordingly, we propose a position-based limited feedback scheme for railway MU-MIMO systems, in which dedicated feedback resource positions are preassigned to codebook vectors. A resource position where users feed back channel quality indicators (CQIs) indicates a special codebook vector. Then, overheads due to precoding matrix index (PMIs) are saved. Even if bandwidth resources assigned to feedback positions may be insufficient to supply every user with a feedback chance, it still has little impact on the total capacity for whether the user with the largest CQI in an active user set is selected in highly populated railway scenarios. Moreover, a novel performance criterion called feedback efficiency is proposed. Simulation results demonstrate that the proposed scheme can achieve higher feedback efficiency compared with the conventional scheme.

Index Terms—Channel quality indicator (CQI), feedback efficiency, limited feedback, multiuser multiple-input multiple-output (MU-MIMO), railway mobile communications.

I. INTRODUCTION

WITH the remarkable progress of the railway industry and mobile Internet, train passengers, particularly those on long-distance journeys, are expecting to use the Internet onboard. In future railway communications, the system architecture is highly likely to be based on the mobile-relay structure

Manuscript received February 2, 2015; accepted December 13, 2015. Date of publication December 22, 2015; date of current version October 13, 2016. This work was supported in part by the 973 Program of China under Grant 2012CB316100, by the National Natural Science Foundation of China under Grants 61471303 and 61210002, by the EU Seventh Framework Programme QUICK Project under Grant PIRSES-GA-2013-612652, and by the EU H2020 ITN 5G Wireless Project under Grant 641985. The review of this paper was coordinated by Prof. H. H. Nguyen.

L. Yan and X. Fang are with the Key Laboratory of Info Coding and Transmission, Southwest Jiaotong University, Chengdu 610031, China (e-mail: liyan12047001@my.swjtu.edu.cn; xmfang@swjtu.edu.cn).

C.-X. Wang is with the Institute of Sensors, Signals, and Systems, School of Engineering and Physical Sciences, Heriot-Watt University, Edinburgh EH14 4AS, U.K. (e-mail: cheng-xiang.wang@hw.ac.uk).

Color versions of one or more of the figures in this paper are available online at <http://ieeexplore.ieee.org>.

Digital Object Identifier 10.1109/TVT.2015.2511021

[1], [2]. This means that users in a train communicate with indoor access points inside train carriages, which are then connected to outdoor antennas to communicate with wayside base stations [3]. This structure can potentially avoid the penetration loss due to train carriages. However, under the present situation, considering the security of train control system, public mobile communication operators are not allowed to be directly involved in railway communications. Hence, it is almost impossible to refit current trains that are in use to adapt to this structure. Nevertheless, public mobile networks along railways provide train passengers with a wireless access opportunity. Therefore, during the transition period of system evolutions, onboard passenger equipment can only directly connect to wayside public mobile networks to get wireless services. Up to now, long-term evolution (LTE) has been applied to public mobile networks [4]. As the most attractive technology that enables larger capacity in LTE networks, multiple-input multiple-output (MIMO) has generated a great deal of research interest in wireless communications [5], [6]. However, due to the limited volume of common user equipment (UE) including the train passenger equipment, it is hard to configure sufficient numbers of antennas in UE to exploit fully the capacity gain of MIMO. To overcome this problem, researchers are turning their attention to the multiuser MIMO (MU-MIMO) technology, which spreads the spatial resources among multiple users to achieve larger capacity [7]–[9]. In this paper, the so-called railway MU-MIMO communication systems are used where the MU-MIMO technology is employed between train passengers and wayside eNodeBs (eNBs).

As UE has limited capability to cancel interference, it is normally the task of eNBs to precode the downlink signals to suppress the interuser interference for MU-MIMO systems. Nevertheless, the channel state information at the transmitter (CSIT), which is fed back by users to convey the downlink channel conditions, is crucial for the given task. The requirement of CSIT poses a bandwidth burden on feedback links. With limited feedback resources, reducing the large-scale concurrent feedback overheads becomes an urgent problem. In [10], a two-step downlink CSI feedback scheme was proposed, in which the first step is to feed back some coarse information for the user selection, and the second step is to feed back precise CSI for the precoding. In [11], a differential CSI feedback scheme was investigated. The given schemes were all studied under public mobile networks. However, for railway scenarios, there are some special characteristics, such as determined running track and highly populated onboard users, which can be properly exploited to find other solutions. Nevertheless, the characteristics have both pros and cons. In high-speed

movement scenarios, the large Doppler effect is always an inevitable problem that needs to be carefully handled. Fortunately, in the special railway scenarios, the characteristics of determined running directions, regular running tracks, and repetitive movements of trains along fixed running tracks lead to a regular, repetitive, and predictable Doppler shift curve, thereby making it easy to track and compensate the Doppler effects [12], [13]. Moreover, there have been several research results focusing on the Doppler effect estimation and compensation for high-speed railway scenarios, such as in [14] and [15]. Based on this observation, in this paper, we assume that the Doppler effect can be perfectly compensated and has almost no influence on the final performance for both the conventional scheme and the proposed scheme, which also ensures the fairness when comparing the performance of two schemes in both theoretical analyses and simulations.

CSI consists of the small-scale fading channel parameters and the large-scale SNR. In practice, considering limited feedback resources, CSI cannot be fed back to the transmitter in the form of exact values. Instead, codebook-based CSI feedback method has generally been used in practical finite-rate feedback systems [16], [17]. For instance, in the conventional MU-MIMO feedback scheme, all UE units first estimate their downlink channel conditions, including channel direction of small-scale fading and large-scale SNRs. Based on the codebook that is offline designed and known both to eNBs and UE units, every UE quantizes its channel direction of small-scale fading to a codebook vector denoted by precoding matrix index (PMI) of size α bits. In addition to PMI, the channel quality indicator (CQI) of size β bits indicating the quantized large-scale SNR is also needed to be fed back to eNBs for the user selection. More details about channel direction and SNR quantization are given in Section III-A and B, respectively. Based on PMI feedback, UE units are divided into different user sets, i.e., UE units that feed back the same PMI are classified into a user set. Let us assume that M antennas are used in an eNB. Then, M sets with mutually orthogonal PMIs, namely, active user sets, are chosen for the following operations. Finally, the UE with the largest CQI value in each active user set is selected as the participant for the MU-MIMO precoding and transmission [18]. In this paper, for simplicity, we take zero-forcing beamforming (ZFBF) as the precoding scheme [19].

In public mobile networks, users are so distributed that their long-term SNRs (i.e., CQIs) are very diverse. Whether the user with the largest CQI in an active user set is selected can directly affect the overall system capacity. However, in railway MU-MIMO scenarios, passengers are located inside a train whereby the distances between users are relatively small compared with the coverage radius of wayside eNBs. In addition, as the size of codebooks (typically 64) is usually larger than the number of train carriages (typically, eight or 16), passengers with the same selected codebook vector (i.e., belonging to the same user set) potentially stay in the same carriage. Consequently, it is reasonable to assume that passenger equipment of a user set has almost the same average SNR, i.e., CQI. It almost makes no difference to select the user with the maximum CQI value among all the users or among a fraction of users in an active user set.

Based on this observation, we propose an efficient position-based limited feedback scheme for railway MU-MIMO communication systems. In this scheme, dedicated feedback resource positions are preassigned to codebook vectors. Similar to conventional MIMO systems whereby codebooks are shared among all the users, the dedicated feedback resources are also shared among all the users in the proposed scheme. Without loss of generality, a resource position can be construed as a specialized frequency point. Nevertheless, it can be any mutually orthogonal resources, such as in time or other domains. To facilitate the understanding, an example is given in the following. Suppose that W codebook vectors make up a codebook, i.e., $C = \{\mathbf{c}_1, \dots, \mathbf{c}_W\}$. Moreover, let $\text{FP} = \{\text{fp}_1, \dots, \text{fp}_W\}$ denote the preassigned feedback positions for these codebook vectors. For \mathbf{c}_j ($j = 1, \dots, W$), its dedicated feedback position is fp_j . If a user quantizes its channel direction of small-scale fading to \mathbf{c}_j , then it will feed back its CQI on fp_j . For an eNB, the resource position, where it receives a user's CQI, has indirectly indicated the quantized codebook vector of this user. In this way, unlike the conventional MU-MIMO feedback scheme (simplified as the "conventional scheme"), overheads due to PMI feedback are avoided in the proposed position-based limited feedback scheme (simplified as the "proposed scheme"), thereby saving feedback costs for finite-rate feedback systems.

In the proposed scheme, bandwidth resources are preassigned to feedback positions, and a position has multiple feedback channels to accommodate multiple users. However, in practice, with limited feedback resources, for some feedback positions, the bandwidth resources may be insufficient to provide every user with a feedback chance. As a result, the user with the maximum CQI value may not get the feedback opportunity, thereby cannot be selected, which will degrade the total system capacity to some extent. Fortunately, in railway MU-MIMO communication systems, passenger equipment in a user set has almost the same CQI. Thus, it would have little impact on the total capacity whether the user with the largest CQI in an active user set is selected in highly populated railway scenarios.

The remainder of this paper is organized as follows. Section II overviews the conventional MU-MIMO feedback scheme and presents the position-based limited feedback scheme. Section III gives the mathematical models. Section IV provides the simulation results. Finally, Section V concludes this paper.

II. POSITION-BASED LIMITED FEEDBACK SCHEME

A. Conventional MU-MIMO Feedback Scheme

In the conventional scheme, to maximize the system capacity, all the UE units are required to feed back their downlink PMIs and CQIs, as shown in Fig. 1(a). Then, based on their feedback, the eNB selects the users with the maximum CQI values in different active user sets and generates the precoding vectors to suppress the interuser interference. It is notable that precoding vectors are different from codebook vectors. The precoding vectors, which are applied to the final transmission,

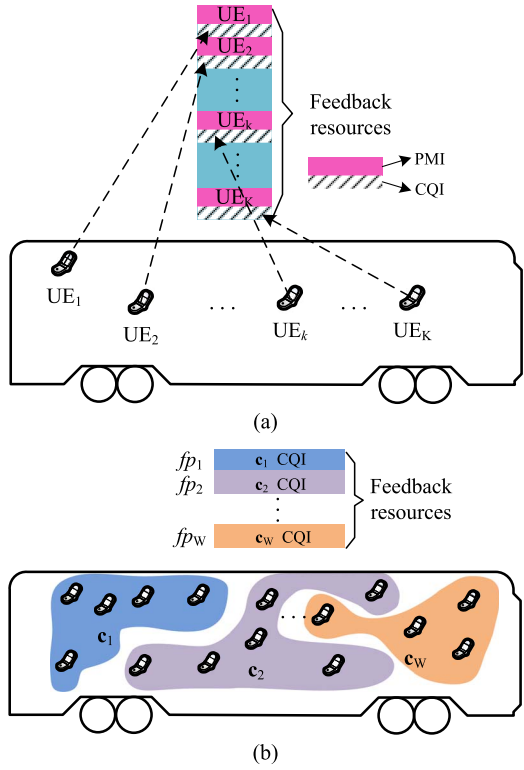


Fig. 1. Feedback scheme comparisons. (a) Feedback resource occupation in the conventional scheme and (b) Feedback resource occupation in the proposed scheme.

are generated according to the codebook vectors fed back by selected users (the user selection and precoding vector generation procedures are detailed in Section III). In practice, the number of all feedback users is much larger than that of users to be selected. Therefore, most feedback bandwidth resources, which are consumed by the users that have fed back their PMIs and CQIs but are not selected, are wasted. This heavily aggravates the feedback burden of finite-rate feedback systems.

B. Proposed Position-Based Limited Feedback Scheme

In railway scenarios, the distribution of passengers in the same carriage is very tight. Hence, it is very possible that passenger equipment in the same carriage is assigned to the same user set. Moreover, as the size of codebooks is usually larger than the number of train carriages, even passengers in the same carriage will be further assigned to different user sets. Consequently, it is reasonable to assume that passenger equipment of a user set has almost the same CQI. Therefore, for an active user set, it almost makes no difference to select the user with the maximum CQI value among all users or among a fraction of all users. Base on this observation, in the proposed scheme, dedicated feedback positions are preassigned to codebook vectors as shown in Fig. 1(b). If the quantized codebook vector is \mathbf{c}_j , then the user will feed back its CQI on the dedicated position fp_j . For an eNB, the resource position, where it receives a user's CQI, indicates the quantized codebook vector of this user. In this way, the feedback bandwidth resources used for the transmission of PMIs are saved.

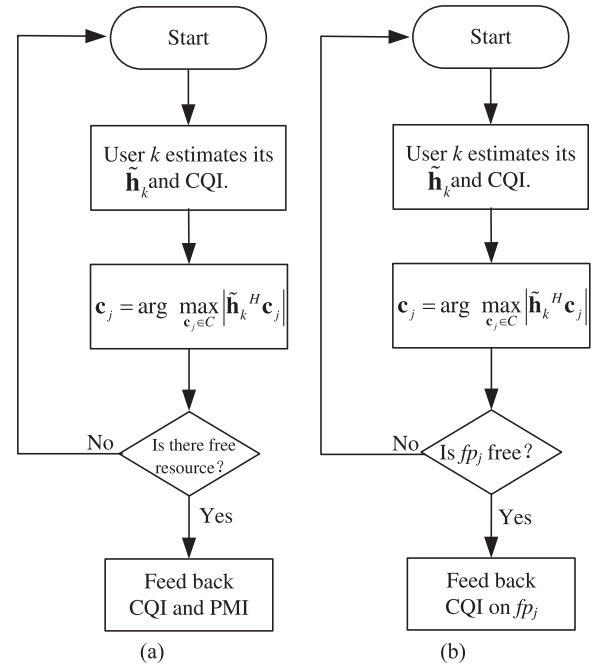


Fig. 2. Feedback procedure comparisons. (a) Conventional scheme and draft-rules online. (b) Proposed scheme.

The detailed feedback procedures of the conventional scheme and the proposed scheme are compared in Fig. 2. In both schemes, a user needs to first estimate the channel direction of small-scale fading $\tilde{\mathbf{h}}_k$ and CQI, and then quantizes $\tilde{\mathbf{h}}_k$ to a codebook vector. In contrast to the conventional scheme, for the proposed scheme, the codebook vector indexes are not needed to be sent to eNBs. Instead, a dedicated feedback resource position is preassigned to a special codebook vector, e.g., fp_j for \mathbf{c}_j . A user only needs to feed back its CQI on a dedicated position assigned to this user's quantized codebook vector. For an eNB, the resource position, where it receives a user's CQI, is able to indicate the quantized codebook vector. In this way, the overheads due to PMIs in the conventional scheme are saved, thereby mitigating the feedback burden of finite-rate feedback systems. With limited feedback resources, for both schemes, there may be the case that not every user can obtain a feedback chance. Nevertheless, for highly populated railway scenarios, it almost has no impact on the total capacity whether the user with the largest CQI in an active user set is selected. Based on this, in the proposed scheme, the resource position, where a user feeds back its CQI, is used to indicate the PMI, thereby saving the resources used by PMI feedback. Note that, in the conventional LTE networks, users' uplink data is scrambled by dedicated cell radio network temporary identifier, which is used to help eNBs to recognize the users [20]. This approach is also applicable in the proposed scheme.

In MIMO systems, a codebook is shared among all the users. Equivalently, the dedicated feedback resources are shared among all the users. However, in practice, there may be inadequate bandwidth resources to distribute to the feedback positions of codebook vectors. Hence, only the users who obtain feedback resources have the opportunity to feed back

their CQIs. This indicates that feedback bandwidth resource competition may be brought in. However, with limited feedback resources, this competition also exists in the conventional scheme. In this paper, for simplicity and fairness, we do not consider feedback collisions for both the proposed scheme and the conventional scheme. Nevertheless, in our future work, we will take feedback collisions into consideration. Although in the given situation, some users, maybe including the one with the largest CQI value, cannot get feedback opportunities, whether the user with the largest CQI in an active user set is selected almost makes no difference for the highly populated railway scenarios, where all passengers in a user set have almost the same CQI value.

It is also possible that some preassigned feedback resources are not occupied, indicating that these resources are wasted. In this situation, most users have the same channel direction of small-scale fading. Consequently, feedback concentrates on some codebook vectors, and the other vectors are not used. Still, only one user out of the users feeding back the same codebook vector can be selected. Then, with the need to feed back PMIs in the conventional scheme, more feedback resources are wasted by those users that have consumed the feedback resources but are not selected. In the proposed scheme, eNBs can adjust the amount of feedback bandwidth resources according to wireless channel conditions and then inform users of the adjustment. For the codebook vectors selected by lots of users in the last subframe, more feedback bandwidth resources can be assigned to them in a subsequent subframe. Otherwise, fewer feedback bandwidth resources should be used. In this way, fewer feedback bandwidth resources are wasted, and more users can obtain the opportunity to feed back their CQIs, thereby further enhancing the capacity.

III. MATHEMATICAL MODELS

In MU-MIMO systems, system capacity and feedback overhead are used as two independent performance criteria. Usually, more feedback overheads produce higher capacity, and *vice versa*. Hence, it is beneficial to combine these two criteria to realize an overall evaluation of MU-MIMO systems. Based on this observation, in this paper, we propose a novel performance criterion called MU-MIMO feedback efficiency. It is defined as the attained downlink capacity per unit feedback overhead and can be written as

$$\Omega = \frac{T_f \sum_{i=1}^M \text{BW}_f \cdot \log_2(1 + \text{SINR}_i)}{\sum_{k=1}^K B_k} \quad (1)$$

where the numerator is the obtained capacity and the denominator is the corresponding consumed feedback bits in one feedback period. Here, K denotes the number of total feedback users. Under the assumption that every user is configured with one receiving antenna and the eNB is configured with M antennas, M out of K users are supposed to be selected for the ZFBF precoding procedure. Moreover, SINR_i is the signal-to-noise-plus-interference ratio (SINR) of the selected user i , and B_k represents the number of total feedback bits of user k . In the conventional scheme, B_k consists of an α -bit PMI and

a β -bit CQI. In contrast, without the need to feed back PMI in the proposed scheme, a β -bit CQI is the whole content of B_k . In LTE networks, the bandwidth represented by a single feedback is semi-statically configured by the higher layer, and it is denoted by BW_f here [21]. For frequency nonselective channels, a wideband feedback, indicating larger observation interval in the frequency domain, is supported. According to [22] and [23], wireless channels in railway scenarios where trains run over viaducts most of the time can be regarded as line of sight (LOS) with large coherence bandwidth. Hence, a wideband feedback with BW_f set to a large value is achievable. In (1), T_f denotes the feedback period. In this paper, the feedback efficiency is calculated based on one feedback period. Then, the units of the numerator and denominator are unified. As stated previously, due to the special characteristics of railway scenarios and the technology developments of Doppler effect estimation and compensation, in this paper, we assume that the Doppler effect can be perfectly compensated in both the conventional scheme and the proposed scheme.

Generally, the small-scale fading of wireless channels can be modeled as the product of its magnitude and direction, i.e.,

$$\mathbf{h} = \|\mathbf{h}\| \cdot \tilde{\mathbf{h}} \quad (2)$$

where $\tilde{\mathbf{h}}$ and $\|\mathbf{h}\|$ represent the channel direction and magnitude, respectively. The lowercase boldface letters are used to express vectors. $\|\cdot\|$ represents the 2-norm operation.

Here, for a selected user i , \mathbf{h}_i is an $M \times 1$ vector. Let x_i denote the transmitted downlink data signal. Then, the received signal can be expressed as [24], [25]

$$y_i = \sqrt{\text{PL}_i} \mathbf{h}_i^H \mathbf{f}_i x_i + \sqrt{\text{PL}_i} \mathbf{h}_i^H \sum_{k \neq i} \mathbf{f}_k x_k + n_i \quad (3)$$

where PL_i is the large-scale path loss, including the train penetration loss, and n_i represents the additive white Gaussian noise. The unit-norm vector \mathbf{f}_i is the ZFBF precoding vector generated for user i by eNBs. The superscript H denotes the Hermitian transpose. For clarity, the desired signal, corresponding to the first term, and the interuser interference, corresponding to the second term, are separately expressed in (3).

A. Channel Direction Quantization

As aforementioned, with consideration of limited feedback resources, quantized channel directions of small-scale fading and large-scale SNR are fed back to the transmitter in practical finite-rate feedback systems. Here, the detailed channel direction quantization is introduced. As for the SNR quantization, it is detailed in the following. Assume that each user has perfect knowledge of \mathbf{h}_i and the channel direction of small-scale fading is quantized to a unit-form vector $\hat{\mathbf{h}}_i$. Then, the channel direction quantization is to choose a vector from a codebook with finite vectors of size $W = 2^\alpha$, i.e.,

$$C = \{\mathbf{c}_1, \dots, \mathbf{c}_W\}, \quad W = 2^\alpha \quad (4)$$

as $\hat{\mathbf{h}}_i = \mathbf{c}_j$ according to

$$\hat{\mathbf{h}}_i = \arg \max_{\mathbf{c}_j \in C} \left| \tilde{\mathbf{h}}_i^H \mathbf{c}_j \right|. \quad (5)$$

TABLE I
MAPPING FROM SNR TO CQI (BLER = 0.1)

CQI index	Modulation	Code rate×1024	SNR threshold (dB)
1	QPSK	78	-9.478
2	QPSK	120	-6.658
3	QPSK	193	-4.098
4	QPSK	308	-1.798
5	QPSK	449	0.339
6	QPSK	602	2.424
7	16QAM	378	4.489
8	16QAM	490	6.367
9	16QAM	616	8.456
10	64QAM	466	10.266
11	64QAM	567	12.218
12	64QAM	666	14.122
13	64QAM	772	15.849
14	64QAM	873	17.786
15	64QAM	948	19.809

Due to the finite number of vectors in a codebook, there exist some differences between the quantized $\hat{\mathbf{h}}_i$ and the real channel direction of small-scale fading \mathbf{h}_i , namely, quantization error. In the conventional scheme, the α -bit index j , namely PMI, is needed to be fed back to eNBs. While in the proposed scheme, these bits are saved. The resource position, where a user feeds back its CQI, has indicated the quantized PMI.

Practically, the number of total feedback users K is much larger than W . This means that multiple users would quantize their channel directions of small-scale fading to the same \mathbf{c}_j . As stated previously, these users are classified into a user set denoted Λ_j . Consequently, K users are finally divided into W user sets denoted $\Pi_1 = \{\Lambda_1, \dots, \Lambda_W\}$.

B. Calculation of SNR

In MU-MIMO systems, a β -bit CQI (in LTE networks, β is equal to 4), which is used to reflect the average large-scale SNR [26], is needed for the user selection procedure. With limited bits to quantize the continuous SNR values to discrete CQI values, mobile stations cannot feed back the exact SNR to eNBs, which will probably cause declines in performance. However, this is beyond the scope of this paper. As an example, the mapping from SNR to CQI values is listed in Table I [26]. In the case that the SNR is too low to bear a transmission, the CQI index is set to 0.

Here, we provide the models to calculate the SNR. According to [26], although in LTE networks, different subcarriers may see different SNRs, link adaptation is not done per-subcarrier because of significant feedback and control signal overheads. Instead, link quality metrics (LQMs) are used to map multiple SNRs of multiple subcarriers to an effective flat SNR. Then, the flat SNR is mapped to CQIs, which means that CQIs can only reflect the average large-scale channel quality. Based on this observation, only the large-scale fading is considered during the calculation of average SNR. Fig. 3 gives the geometric architecture to assist the following formula derivation of SNR, where R is the coverage radius of eNBs, d_{\min} is the vertical distance between the track and eNBs, L_t is the length of the train, and the abscissa axis denotes the moving direction of a train with the original point set at the projection of eNBs on the

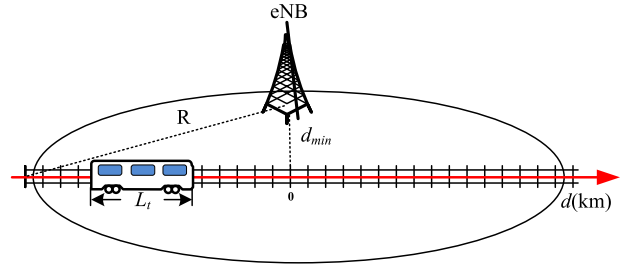


Fig. 3. Geometric architecture for SNR calculation.

track. The front of the train is set as the reference point, i.e., d is equal to 0 when the front of train is at the original point.

For simplicity, it is assumed that the total transmit power of eNBs, which is denoted P , is equally distributed to all selected users, i.e., $E[|x_i|^2] = P/M$, where $E[\cdot]$ denotes the statistical expectation. Without loss of generality, the SNR_i in decibels of user i with a signal propagation distance d can be expressed as

$$\text{SNR}_i(d) = P_r(d) - A - N_0 \tag{6}$$

where N_0 is the power of AWGN. A is the train penetration loss, and $P_r(d)$ is the received signal strength, which can be modeled as [27]

$$P_r(d) = P_t - \text{PL}(d) + X_{\sigma_{\text{dB}}} \tag{7}$$

where P_t is the transmit power in decibels, which is equal to $10 \lg(P/M)$. $\text{PL}(d)$ is the path loss with signal propagation distance d . $X_{\sigma_{\text{dB}}}$ is the lognormal distributed shadow fading with mean 0 and standard derivation σ_{dB} . It is easy to get that $\text{SNR}_i(d) \sim N(m(d), \sigma_{\text{dB}}^2)$, where $m(d)$ is the average SNR, which is expressed as

$$m(d) = P_t - \text{PL}(d) - A - N_0. \tag{8}$$

Based on the given analysis, we can obtain the average SNR and CQI comparisons between the front and the rear of the train as shown in Fig. 4. Detailed simulation parameters are listed in Table II. As shown in Fig. 4(a), since the length of the train is much smaller than the coverage radius of the eNB, the average SNR difference between the front and the rear of the train is very small when the train is far from the eNB. As the train moves towards the eNB, the difference becomes obvious. However, after the average SNR is mapped to CQI, the CQI gap is greatly reduced as shown in Fig. 4(b). Compared with the whole train (typically, it is around 200 m or 400 m), the length of a carriage (typically, it is around 25 m) is much smaller. Hence, it is very possible that users in the same carriage have almost the same CQI. As aforementioned, considering the limited feedback resources, a random small-scale fading channel is first quantized to a codebook vector and then the index of this codebook vector is fed back to eNBs. Equivalently, all random small-scale fading channels are finally divided into a finite number of codebook vectors. Hence, users, who actually have different small-scale channels but quantize them to the same codebook vector, seem to experience the same small-scale fading from the view of eNBs. As the size of a codebook is

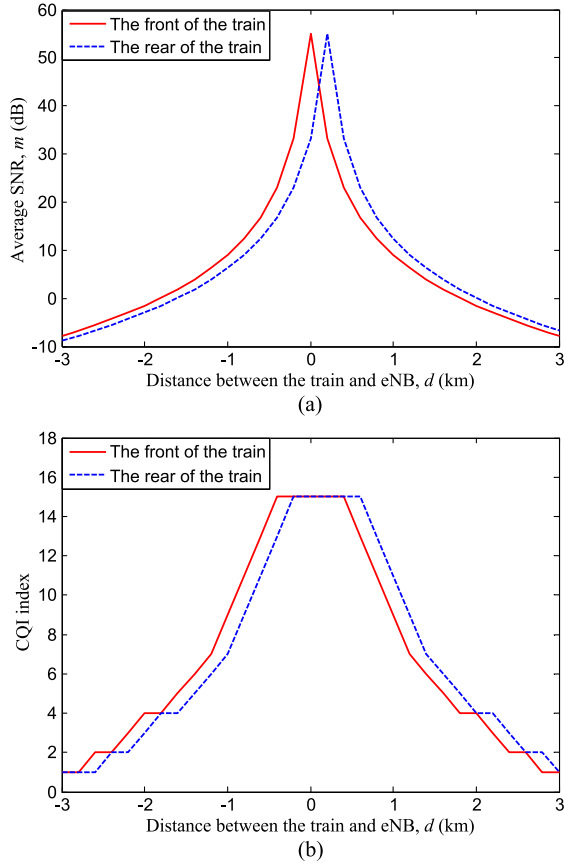


Fig. 4. Comparisons between the front and the rear of the train. (a) Average SNR comparison and (b) CQI comparison.

TABLE II
SIMULATION PARAMETERS [27], [28]

Parameters	Values
Number of feedback UEs K	500(total passengers) $\times 40\%$ (activation rate)
Number of antennas in eNB M	4
Number of bits for PMI α	6
Number of bits for CQI β	4
Feedback period T_f	1ms
Power of Noise N_0	-174dBm/Hz
Train penetration loss A	20dB[2]
Central frequency	2GHz
Feedback frequency interval BW_f	0.5MHz
Transmit power of eNB P	20W
Coverage radius of eNB R	3km
Vertical distance between eNB and track d_{min}	50m
The length of the train	200m
Large-scale path loss model	Hata

larger than the number of train carriages, it is very possible that passengers in the same carriage will be further assigned to different user sets. Hence, it is reasonable to assume that passengers in the same user set have almost the same CQI.

C. User Selection Algorithm

Based on the PMIs and CQIs fed back from all the users, eNBs conduct the user selection to support up to M out of K users in the subsequent ZFBF precoding. To simplify the analysis, we use the semi-orthogonal user selection algorithm [28]. eNBs select the first user from the whole user set $\Pi_1 = \{\Lambda_1, \dots, \Lambda_W\}$ as

$$u_1 = \arg \max_{k \in \Pi_1} \text{SNR}_k. \quad (9)$$

If the first user comes from $\Lambda_{(1)}$ (for simplicity, the selected active user sets are reordered, i.e., the i th selected active user set is denoted $\Lambda_{(i)}$), then the $(i+1)$ th user will be selected from

$$\Pi_{i+1} = \Pi_i - \Lambda_{(i)} - \left\{ \Lambda_j : \left| \hat{\mathbf{h}}_{\Lambda_j}^H \hat{\mathbf{h}}_{\Lambda_{(i)}} \right| \leq \delta, \Lambda_j \in \Pi_i - \Lambda_{(i)} \right\} \quad (10)$$

as

$$u_{i+1} = \arg \max_{k \in \Pi_{i+1}} \text{SNR}_k \quad (11)$$

where δ is a threshold that indicates the maximum allowable spatial correlation between the selected codebook vectors for subsequent linear beamforming.

D. ZFBF Precoding Algorithm

After the given user selection procedure, M out of K users, making up a new user set U , are selected for the ZFBF precoding algorithm. For user i , where $i \in U$, the generated ZFBF precoding vector \mathbf{f}_k must satisfy

$$\hat{\mathbf{h}}_i^H \cdot \mathbf{f}_k = 0 \quad \text{for } k \neq i, \quad k \in U. \quad (12)$$

However, as discussed before, due to the quantization error on $\hat{\mathbf{h}}_i$, the generated ZFBF precoding vector is not thoroughly orthogonal to the real channel direction \mathbf{h}_i . In other words, there exists interuser interference, under which the SINR of user i can be modeled as

$$\begin{aligned} \text{SINR}_i &= \frac{\text{PL}_i \frac{P}{M} |\mathbf{h}_i^H \mathbf{f}_i|^2}{N_0 + \text{PL}_i \frac{P}{M} \sum_{k \neq i} |\mathbf{h}_i^H \mathbf{f}_k|^2} \\ &= \frac{\|\mathbf{h}_i\|^2 |\tilde{\mathbf{h}}_i^H \mathbf{f}_i|^2}{10^{-\text{SNR}_i[\text{dB}]/10} + \|\mathbf{h}_i\|^2 \sum_{k \neq i} |\tilde{\mathbf{h}}_i^H \mathbf{f}_k|^2}. \end{aligned} \quad (13)$$

According to [28], [29], (13) can be further rewritten as (14), shown at the bottom of page. It is shown in [28] that the

$$\text{SINR}_i = \frac{\|\mathbf{h}_i\|^2 \beta(1, M-1)}{10^{-\text{SNR}_i[\text{dB}]/10} + \|\mathbf{h}_i\|^2 \left(1 - |\tilde{\mathbf{h}}_i^H \hat{\mathbf{h}}_i|^2\right) \sum_{k \neq i} \beta(1, M-2)}. \quad (14)$$

distribution of $1 - |\tilde{\mathbf{h}}_i^H \hat{\mathbf{h}}_i|^2$ with a well-designed codebook of size 2^α is as follows:

$$f_{1-|\tilde{\mathbf{h}}_i^H \hat{\mathbf{h}}_i|^2}(x) = \begin{cases} 2^\alpha x^{M-1}, & 0 \leq x \leq 2^{-\frac{\alpha}{M-1}} \\ 1, & x > 2^{-\frac{\alpha}{M-1}}. \end{cases} \quad (15)$$

As a result, we can get [28], [30], [31]

$$E[\text{SINR}_i] = \frac{1}{10^{-E[\text{SNR}_i[\text{dB}]]/10} + (M-1)2^{-\frac{\alpha}{M-1}}}. \quad (16)$$

From (16), we can see that with SNR increasing, the value of $E[\text{SINR}_i]$ mainly depends on the interuser interference. In other words, the MU-MIMO communication system is interference limited, which has been investigated in [28], [30], and [31].

E. Ω of the Conventional Feedback Scheme

For simplicity, it is assumed that passengers uniformly distribute in a train. Then, for every codebook vector, there are $L = K/W$ users to feed back their indexes, where L is defined as the user selection gain here. From the user selection procedure, we can see that all the selected users for the ZFBF precoding have the maximum CQI values out of the corresponding active user sets. With L users feeding back their CQIs, the cumulative distribution function of the maximum CQI value, i.e., $\text{SNR}_{\max} = \max\{\text{SNR}_1, \dots, \text{SNR}_L\}$ is

$$F_{\text{SNR}_{\max}}(z) = F^L_{\text{SNR}}(z). \quad (17)$$

Correspondingly, the probability density function (pdf) of (17) can be derived as

$$f_{\text{SNR}_{\max}}(z) = L \cdot F^{L-1}_{\text{SNR}}(z) \cdot f_{\text{SNR}}(z) \quad (18)$$

where $F_{\text{SNR}}(z)$ with SNR in decibels can be expressed as

$$\begin{aligned} F_{\text{SNR}}(z) &= \int_{-\infty}^z \frac{1}{\sigma_{\text{dB}} \sqrt{2\pi}} e^{-\frac{(t-m)^2}{2\sigma_{\text{dB}}^2}} dt \\ &= \Phi\left(\frac{z-m}{\sigma_{\text{dB}}}\right). \end{aligned} \quad (19)$$

Then, the expectation of the maximum SNR in the conventional scheme can be calculated as

$$\begin{aligned} E[\text{SNR}_{\max, \text{con}}] &= \int_{-\infty}^{\infty} z f_{\text{SNR}_{\max}}(z) dz \\ &= \int_{-\infty}^{\infty} z \cdot L \cdot F^{L-1}_{\text{SNR}}(z) \cdot f_{\text{SNR}}(z) dz \\ &= L \int_{-\infty}^{\infty} \frac{z}{\sigma_{\text{dB}} \sqrt{2\pi}} \cdot \Phi^{L-1}\left(\frac{z-m}{\sigma_{\text{dB}}}\right) \\ &\quad \cdot e^{-\frac{(z-m)^2}{2\sigma_{\text{dB}}^2}} dz. \end{aligned} \quad (20)$$

With (20), the obtained average system capacity in the conventional scheme can be expressed as

$$\begin{aligned} E[C_{\text{con}}] &= E\left[\sum_{i=1}^M \text{BW}_f \cdot \log_2(1 + \text{SINR}_i)\right] \\ &= M \times \text{BW}_f \\ &\quad \times \log_2\left(1 + \frac{1}{10^{-E[\text{SNR}_{\max, \text{con}}[\text{dB}]]/10} + (M-1)2^{-\frac{\alpha}{M-1}}}\right). \end{aligned} \quad (21)$$

In the conventional scheme, users require to feed back both PMIs of size α bits and CQIs of size β bits. Based on (1), the feedback efficiency of the conventional scheme can be expressed as

$$\Omega_{\text{con}} = \frac{T_f E[C_{\text{con}}]}{K(\alpha + \beta)}. \quad (22)$$

F. Ω of the Proposed Feedback Scheme

In the proposed scheme, with preassigned resources for feedback, the user selection gain may be different from that of the conventional scheme for some active user sets. Here, we use g to represent the user selection gain for the proposed scheme. Correspondingly

$$E[\text{SNR}_{\max, \text{pro}}] = g \int_{-\infty}^{\infty} \frac{z}{\sigma_{\text{dB}} \sqrt{2\pi}} \times \Phi^{g-1}\left(\frac{z-m}{\sigma_{\text{dB}}}\right) e^{-\frac{(z-m)^2}{2\sigma_{\text{dB}}^2}} dz \quad (23)$$

$$E[C_{\text{pro}}] = M \times \text{BW}_f$$

$$\times \log_2\left(1 + \frac{1}{10^{-E[\text{SNR}_{\max, \text{pro}}[\text{dB}]]/10} + (M-1)2^{-\frac{\alpha}{M-1}}}\right). \quad (24)$$

As stated previously, overheads due to PMIs are saved in the proposed scheme. Only the CQI of size β bits is needed to be fed back to eNBs. Then, the feedback efficiency of the proposed scheme is

$$\Omega_{\text{pro}} = \frac{T_f E[C_{\text{pro}}]}{Wg\beta}. \quad (25)$$

Obviously, compared with the conventional scheme, $K\alpha + (K - Wg)\beta$ feedback bits are saved in the proposed MU-MIMO feedback scheme.

IV. NUMERICAL RESULTS

Here, we conduct performance comparisons between the conventional and proposed schemes under two different condition settings. The first condition setting is that two schemes host the same number of feedback users, i.e., $L = g$. In contrast, under the second condition setting, similar available feedback bits are distributed to these two schemes. Fig. 5 shows the

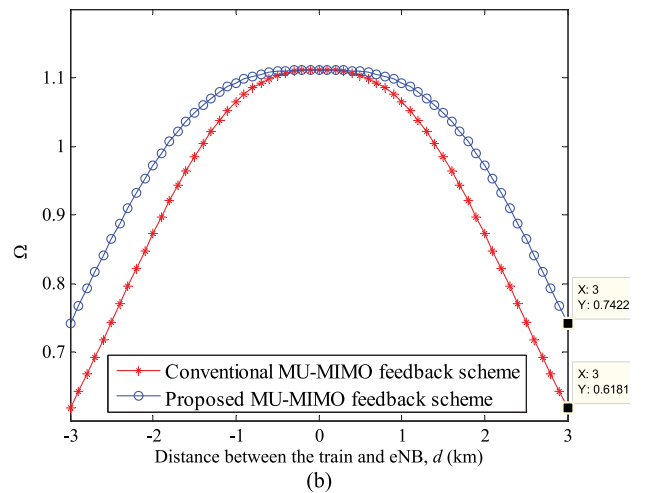
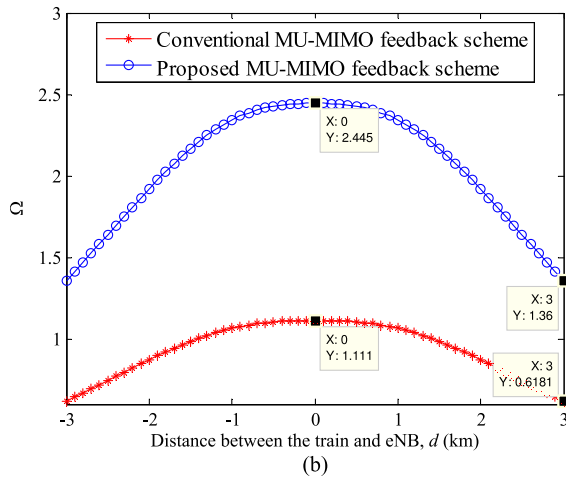
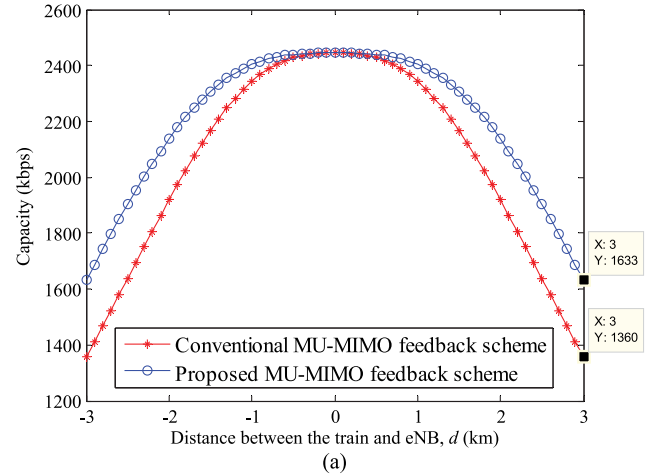
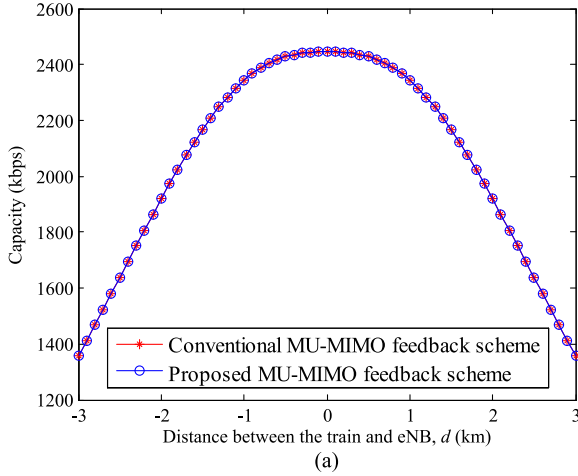


Fig. 5. Performance comparisons under the first condition setting. (a) Capacity comparison and (b) feedback efficiency comparison.

Fig. 6. Performance comparisons under the second condition setting: (a) capacity comparison and (b) feedback efficiency comparison.

performance comparison of two schemes under the first condition setting. As an example for analysis, the detailed simulation parameters are listed in Table II. Since two schemes host the same number of feedback users, they have identical user selection gain, thereby reaching the same system capacity as shown in Fig. 5(a), where two curves are overlapped. With the same capacity, the numerators of Ω_{pro} and Ω_{con} are similar. Although, under the first condition, setting two schemes can obtain the same capacity, fewer feedback resources are needed to reach this capacity for the proposed scheme. In the proposed scheme, the PMI of size α bits is saved. Hence, the denominator of Ω_{pro} is much smaller than that of Ω_{con} . Consequently, the proposed scheme attains higher feedback efficiency as shown in Fig. 5(b). As the consumed feedback resources do not vary with d , i.e., the denominators of Ω_{pro} and Ω_{con} are constant, the performance improvement is also constant. From the points at $d = 3$ km and $d = 0$, we can get that the performance gain is about 1.2 times.

In Fig. 6, the performance comparison is conducted under the second condition setting of similar feedback resources. As we have analyzed earlier, compared with the conventional scheme, $Ka + (K - Wg)\beta$ feedback bits are saved in the proposed scheme. More precisely, these bits can be used to accommodate more feedback users to enable larger user selection

gain. The number of extra admissible users are $\lfloor (Ka + (K - Wg)\beta)/W\beta \rfloor$, and thereby, $g = L + \lfloor (Ka + (K - Wg)\beta)/W\beta \rfloor$, where $\lfloor \cdot \rfloor$ denotes the round down operator. With more admissible users to feed back in the proposed scheme, a better capacity performance is obtained as shown in Fig. 6(a). As aforementioned, with SNR increasing, MU-MIMO systems become interference limited, i.e., the capacity performance primarily depends on the interuser interference. Because of that, with the train closing to eNB, the performance gap between two schemes is gradually reduced. At the center area of eNBs with high SNR [i.e., the original point in Fig. 6(a)], the capacity of two schemes is even the same. Fig. 6(b) shows the corresponding feedback efficiency. Under the second condition setting, the same feedback bits are assigned to two schemes. Hence, Ω_{pro} and Ω_{con} have the same denominator, and the feedback efficiency curves in Fig. 6(b) have the same trend as that of the capacity curves in Fig. 6(a). From the point at $d = 3$ km, we can get that the maximum performance gain is about 0.2 times. As the codebook size W is usually larger than the antenna number M , some feedback bits are wasted by the users who choose the vectors that are not finally selected by the eNB. Hence, the saved $Ka + (K - Wg)\beta$ feedback bits do not produce obvious capacity gain.

V. CONCLUSION

In this paper, to reduce the feedback costs, we have proposed an efficient position-based limited feedback scheme for railway MU-MIMO scenarios where passenger equipment assigned to a user set almost have the same CQI. In this scheme, dedicated feedback resource positions are preassigned to codebook vectors. After quantizing the channel direction of small-scale fading to a codebook vector, the user feeds back its CQI on the dedicated position preassigned to this codebook vector. In this way, overheads due to PMIs in the conventional scheme can be saved. Although there may be a situation in which the bandwidth resources assigned to feedback positions are not sufficient to support all the users to feed back their CQIs, it almost makes no difference whether we select the user with the largest CQI value among all users or a fraction of all users of an active user set in highly populated railway scenarios. Moreover, a new performance criterion called feedback efficiency has been developed. The theoretical analysis and simulation results have revealed that, compared with the conventional scheme, the proposed scheme can attain higher feedback efficiency with the same number of total feedback users or can achieve larger capacity with the same feedback bits.

REFERENCES

- [1] C.-X. Wang *et al.*, "Cellular architecture and key technologies for 5G wireless communication networks," *IEEE Commun. Mag.*, vol. 52, no. 2, pp. 122–130, Feb. 2014.
- [2] L. Chen *et al.*, "Mobile relay in LTE-advanced systems," *IEEE Commun. Mag.*, vol. 51, no. 11, pp. 144–151, Nov. 2013.
- [3] X. Zhu, S. Chen, H. Hu, X. Su, and Y. Shi, "TDD-based mobile communication solutions for high-speed railway scenarios," *IEEE Wireless Commun.*, vol. 20, no. 6, pp. 22–29, Dec. 2013.
- [4] H. Ekstrom *et al.*, "Technical solutions for the 3G long-term evolution," *IEEE Commun. Mag.*, vol. 44, no. 3, pp. 38–45, Mar. 2006.
- [5] W. Luo, X. Fang, M. Cheng, and Y. Zhao, "Efficient Multiple-Group Multiple-Antenna (MGMA) scheme for high-speed railway viaducts," *IEEE Trans. Veh. Technol.*, vol. 62, no. 6, pp. 2558–2569, Jul. 2013.
- [6] L. Juho and H. Jin-Kyu, "MIMO technologies in 3GPP LTE and LTE-advanced," *EURASIP J. Wireless Commun. Netw.*, vol. 2009, 2009, Art. ID 302092.
- [7] J. Duplity *et al.*, "MU-MIMO in LTE systems," *EURASIP J. Wireless Commun. Netw.*, vol. 2011, no. 1, 2011, Art. ID 496763.
- [8] S. Ramprasad and A. Benjebbour, "MU-MIMO in LTE: Performance and the challenges for future enhancement," in *Proc. IEEE ICC*, Ottawa, ON, Canada, Jun. 2012, pp. 6959–6965.
- [9] L. Liu *et al.*, "Downlink MIMO in LTE-advanced: SU-MIMO vs. MU-MIMO," *IEEE Commun. Mag.*, vol. 50, no. 2, pp. 140–147, Feb. 2012.
- [10] I. Sohn, C. S. Park, and K. B. Lee, "Downlink multiuser MIMO systems with adaptive feedback rate," *IEEE Trans. Veh. Technol.*, vol. 61, no. 3, pp. 1445–1451, Mar. 2012.
- [11] X. Li, N. Park, and Y. Kim, "Differential precoding scheme of LTE systems over temporally correlated channels," in *Proc. IEEE Int. Conf. Veh. Technol.*, San Francisco, CA, USA, Sep. 2011, pp. 1–5.
- [12] Y. Zhou, "Radio environment map based maximum a posteriori Doppler shift estimation for LTE-R," in *Proc. IEEE HMWC*, Beijing, China, Nov. 2014, pp. 5–5.
- [13] Y. Zhao, C. Yin, and J. Li, "Learning-and optimization-based channel estimation for cognitive high-speed rail broadband wireless communications," *Proc. IEEE ISCIT*, Gold Coast, Qld., Australia, Oct. 2012, pp. 562–567.
- [14] H. Cheon, "Frequency offset estimation for high speed users in E-UTRA uplink," in *Proc. IEEE Int. Conf. Pers., Indoor Mobile Radio Commun.*, Athens, Greece, Sep. 2007, pp. 1–5.
- [15] Q. Du, G. Wu, Q. Yu, and S. Li, "ICI mitigation by Doppler frequency shift estimation and pre-compensation in LTE-R systems," in *Proc. IEEE ICC*, Beijing, China, Aug. 2012, pp. 469–474.
- [16] M. Trivellato, F. Boccardi, and H. Huang, "On transceiver design and channel quantization for downlink multiuser MIMO systems with limited feedback," *IEEE J. Sel. Areas Commun.*, vol. 26, no. 8, pp. 1494–1504, Oct. 2008.
- [17] D. Love *et al.*, "An overview of limited feedback in wireless communication systems," *IEEE J. Sel. Areas Commun.*, vol. 26, no. 8, pp. 1341–1365, Oct. 2008.
- [18] P. Frank, A. Muller, and J. Speidel, "Fair performance comparison between CQI and CSI based MU-MIMO for the LTE downlink," in *Proc. IEEE EW*, Lucca, Italy, Apr. 2010, pp. 93–98.
- [19] E.-H. Shin and D. Kim, "On the optimal sum-capacity growth of ZFBF with quality based channel reporting in multiuser downlink channels," *IEEE Trans. Commun.*, vol. 57, no. 6, pp. 1643–1647, Jun. 2009.
- [20] *Evolved Universal Terrestrial Radio Access (E-UTRA), Medium Access Control (MAC) Protocol Specification*, 3GPP TS 36.321, V11.0.0, 2012.
- [21] *Evolved Universal Terrestrial Radio Access (E-UTRA), Physical Layer Procedures*, 3GPP TS 36.213, V9.3.0, 2010.
- [22] L. Liu *et al.*, "Position-based modeling for wireless channel on high-speed railway under a viaduct at 2.35 GHz," *IEEE J. Sel. Areas Commun.*, vol. 30, no. 4, pp. 834–845, May 2012.
- [23] A. Ghazal, C.-X. Wang, B. Ai, D. Yuan, and H. Haas, "A nonstationary wideband MIMO channel model for high-mobility intelligent transportation systems," *IEEE Trans. Intell. Transp. Syst.*, vol. 16, no. 1, pp. 1–13, Feb. 2015.
- [24] Y. Du, J. Tong, J. Zhang, and S. Liu, "Evaluation of PMI feedback schemes for MU-MIMO pairing," *IEEE Syst. J.*, vol. 4, no. 4, pp. 505–510, Dec. 2010.
- [25] B. Badic, R. Balraj, T. Scholand, Z. Bai, and S. Iwelski, "Impact of feedback and user pairing schemes on receiver performance in MU-MIMO LTE systems," in *Proc. IEEE WCNC*, Shanghai, China, Apr. 2012, pp. 399–403.
- [26] J. Francis and N. Mehta, "EESM-based link adaptation in OFDM: Modeling and analysis," in *Proc. IEEE GLOBECOM*, Atlanta, GA, USA, Dec. 2013, pp. 3703–3708.
- [27] M. Cheng, X. Fang, and W. Luo, "Beamforming and positioning-assisted handover scheme for long-term evolution system in high-speed railway," *IET Commun.*, vol. 6, no. 15, pp. 2335–2340, Oct. 2012.
- [28] T. Yoo, N. Jindal, and A. Goldsmith, "Multi-antenna downlink channels with limited feedback and user selection," *IEEE J. Sel. Areas Commun.*, vol. 25, no. 7, pp. 1478–1491, Sep. 2007.
- [29] N. Jindal, "MIMO broadcast channels with finite-rate feedback," *IEEE Trans. Inf. Theory*, vol. 52, no. 11, pp. 5045–5060, Nov. 2006.
- [30] W. Xu, C. Zhao, and Z. Ding, "Limited feedback design for MIMO broadcast channels with ARQ mechanism," *IEEE Trans. Wireless Commun.*, vol. 8, no. 4, pp. 2132–2141, Apr. 2009.
- [31] W. Xu, C. Zhao, and Z. Ding, "Optimisation of limited feedback design for heterogeneous users in multi-antenna downlinks," *IET Commun.*, vol. 3, no. 11, pp. 1724–1735, Nov. 2009.



Li Yan (S'15) received the B.E. degree in communication engineering in 2012 from Southwest Jiaotong University, Chengdu, China, where she is currently working toward the Ph.D. degree with the Key Laboratory of Information Coding and Transmission, School of Information Science and Technology.

Her research interests include handover, network architecture, and reliable wireless communication for high-speed railways.



Xuming Fang (M'00) received the B.E. degree in electrical engineering, the M.E. degree in computer engineering, and the Ph.D. degree in communication engineering from Southwest Jiaotong University, Chengdu, China, in 1984, 1989, and 1999, respectively.

In September 1984, he was a Faculty Member with the Department of Electrical Engineering, Tongji University, Shanghai, China. In 1998 and 1999, he held visiting positions with the Institute of Railway Technology, Technical University at Berlin, Berlin, Germany, and in 2000 and 2001, he was with the Center for Advanced Telecommunication Systems and Services, University of Texas at Dallas, Richardson, TX, USA. Since 2001, he has been a Professor and, since 2006, the Chair of the Department of Communication Engineering with the School of Information Science and Technology, Southwest Jiaotong University. He has, to his credit, around 200 high-quality research papers in journals and conference publications. He is the author or coauthor of five books or textbooks. His research interests include wireless broadband access control, radio resource management, multihop relay networks, and broadband wireless access for high-speed railways.

Dr. Fang is the Chair of the Chengdu chapter of the IEEE Vehicular Technology Society.



Cheng-Xiang Wang (SM'08) received the B.Sc. and M.Eng. degrees in communication and information systems from Shandong University, Jinan, China, in 1997 and 2000, respectively, and the Ph.D. degree in wireless communications from Aalborg University, Aalborg, Denmark, in 2004.

From 2000 to 2001, he was a Research Assistant with the Technical University of Hamburg, Hamburg, Germany. From 2001 to 2005, he was a Research Fellow with the University of Agder, Grimstad, Norway. In 2004, he was a Visiting Researcher with Siemens AG-Mobile Phones, Munich, Germany. Since 2005, he has been with Heriot-Watt University, Edinburgh, U.K., where he became a Professor of wireless communications in 2011. He is also an Honorary Fellow of the University of Edinburgh, a Chair Professor of Shandong University, and a Guest Professor with Southeast University, Nanjing, China. He is the editor of one book and has published one book chapter and over 210 papers in refereed journals and conference proceedings. His current research interests include wireless channel modeling and fifth-generation wireless communication networks, including green communications, cognitive radio networks, high-mobility communication networks, massive multiple-input multiple-output, millimeter-wave communications, and visible light communications.

Dr. Wang served or is serving as a Technical Program Committee (TPC) member, a TPC Chair, and a General Chair for over 70 international conferences. He also served or is currently serving as an Editor for eight international journals, including the IEEE TRANSACTIONS ON VEHICULAR TECHNOLOGY (2011–present) and the IEEE TRANSACTIONS ON WIRELESS COMMUNICATIONS (2007–2009). He was the leading Guest Editor for the IEEE JOURNAL ON SELECTED AREAS IN COMMUNICATIONS Special Issue on Vehicular Communications and Networks. He received Best Paper Awards at the 2010 IEEE Global Communications Conference, the 2011 IEEE International Conference on Communication Technology, the 2012 IEEE International Conference on ITS Telecommunications, and the 2013 Fall IEEE Vehicular Technology Conference. He is a Fellow of the Institution of Engineering and Technology and the Higher Education Academy and a member of Engineering and Physical Sciences Research Council Peer Review College.